Performance Analysis of a Particularly Simple Kalman Filter

Peter S. Maybeck*
Air Force Institute of Technology, Wright-Patterson Air Force Base, Ohio

Because of stringent storage restrictions, a very simple Kalman filter has been proposed for optimally aiding a strapdown inertial navigation system (INS) with data from a radiometric area correlator (RAC) onboard a weapon system currently under development. However, the adequacy of two decoupled three-state filters to meet performance specifications was subject to serious question. A set of covariance analyses has been conducted to determine estimation capabilities in a realistic environment generated by accurate "truth models" of the error characteristics of two competing inertial systems (one using laser gyros and the other, conventional dry gyros) and the RAC system. Despite the simple form, the filters performed well enough to meet system specifications on navigation errors. Because of its extreme precision at low altitudes, the RAC was the dominant factor in attaining this accuracy, with the laser gyro INS providing somewhat better performance than the dry gyro system. Sensitivity analyses revealed that better RAC hardware or RAC error models in the filters would provide the most effective performance enhancement.

Introduction

CURRENTLY the Air Force is developing tactical weapon systems that will afford precision standoff delivery of ordnance. One such system is a glide vehicle with midcourse and terminal navigation and guidance accomplished through use of a strapdown inertial navigation system (INS) aided by a radiometric area correlator (RAC).

Two different low-cost strapdown inertial systems are competing for implementation. Although both use conventional accelerometers to measure specific force, one INS employs laser gyroscopes to measure angular rates, while the other uses conventional dry gyros. This difference will be seen to have a significant impact on the two systems' error characteristics and on Kalman filter performance capabilities.

As the glide vehicle flies a desired trajectory, the RAC provides a number of accurate position fixes by correlating a radiometric "picture" of the terrain immediately below the vehicle with a prestored reference map of that region. The number of such fixes is limited by the amount of computer memory allotted for the reference maps, five or six being a practical upper bound.

A Kalman filter has been designed[1] to combine the information received from the INS and RAC, to estimate the errors being committed by the INS, and to feed back corrective signals to remove these estimated errors. Because of the restricted amount of computer memory allocated to the Kalman filter (less than 1000 words), the proposed design is very simple – two decoupled three-state filters. However, the adequacy of such a simple design to meet performance specifications was subject to significant question, so a covariance analysis has been conducted to determine estimation precision capabilities in a realistic environment.

The next section depicts the Kalman filter design to be evaluated. Then the covariance analysis method is briefly described, and the "truth models" (very complete linear models of the error characteristics of the two inertial systems and the RAC) required by this analysis are developed in detail. Subsequently, the performance capabilities of the proposed design are analyzed, including discussions of filter tuning, estimation error budgets, and sensitivity to parameter variations.

Certain aspects of this study, such as RAC performance characteristics and a detailed portrayal of the glide vehicle trajectory (basically a nonmaneuvering glide with terminal pitchover and descent), are not available for public release at this time. For this reason, the analysis results are presented in the form of percentages or unscaled graphs.

Received Nov. 15, 1977; revision received May 1, 1978.

Index categories: Guidance and Control; Computer Communications, Information Processing and Software; Sensor Systems.

*Associate Professor, Dept. of Electrical Engineering. Member AIAA.

Kalman Filter Design

The proposed design is actually composed of two decoupled, three-state Kalman filters, each maintaining estimates of the INS position, velocity, and attitude angle error states along a single coordinate direction (east and north are the chosen axes). Thus, the six state variables being estimated are δx_e, δx_n – east and north components of the error in the INS-indicated position; δv_e, δv_e – errors in INS-indicated velocity; ϕ_e, ϕ_n – errors in INS-indicated attitude (tilts).

The dynamics model upon which the filters are based is

$$\begin{bmatrix} \dot{\delta x}_e \\ \dot{\delta v}_e \\ \dot{\phi}_n \end{bmatrix} = \begin{bmatrix} 0 & 1 & 0 \\ 0 & 0 & -g \\ 0 & 1/R_0 & 0 \end{bmatrix} \begin{bmatrix} \delta x_e \\ \delta v_e \\ \phi_n \end{bmatrix} + \begin{bmatrix} 0 & 0 \\ 1 & 0 \\ 0 & 1 \end{bmatrix} \begin{bmatrix} w_{e1} \\ w_{e2} \end{bmatrix} \quad (1)$$

and a similar model for δx_n, δv_n, and ϕ_e. In this equation, g is the magnitude of gravity and R_0 is the equatorial radius of the Earth. The driving term w_{e1} is a white Gaussian noise to model acceleration-level errors, and w_{e2} is an independent Gaussian noise to model errors associated with attitude error angular rates. This equation is in the form:

$$\dot{x}(t) = Fx(t) + Gw(t) \quad (2)$$

i.e., a linear, constant coefficient, stochastic differential equation driven by stationary zero-mean white Gaussian noise with autocorrelation

$$E\{w(t)w^t(t')\} = Q\delta(t-t') \quad (3)$$

The sampled-data measurements made available to the filter algorithms are generated by differencing INS-indicated position and RAC-indicated position. For instance, INS-

indicated east position would be the true position plus the error state δx_e:

$$x_{e\text{-INS}} = x_{e\text{-TRUE}} + \delta x_e \tag{4}$$

whereas the RAC-indicated east position would be modeled as the true position corrupted by white Gaussian noise v:

$$x_{e\text{-RAC}} = x_{e\text{-TRUE}} - v \tag{5}$$

Differencing Eqs. (4) and (5) at sample time t_i yields

$$\begin{aligned} z(t_i) &= x_{e\text{-INS}}(t_i) - x_{e\text{-RAC}}(t_i) \\ &= \delta x_e(t_i) + v(t_i) \\ &= [1\ 0\ 0] \begin{bmatrix} \delta x_e(t_i) \\ \delta v_e(t_i) \\ \phi_n(t_i) \end{bmatrix} + v(t_i) \end{aligned} \tag{6}$$

This equation and the corresponding result for the difference of north position indications are of the form:

$$z(t_i) = \boldsymbol{H}\boldsymbol{x}(t_i) + v(t_i) \tag{7}$$

with v being a scalar discrete-time zero-mean white Gaussian noise with time-varying autocorrelation

$$E\{v(t_i)v(t_j)\} = \begin{cases} R(t_i) & t_i = t_j \\ 0 & t_i \neq t_j \end{cases} \tag{8}$$

Formulation of a viable system representation as a pair of independent three-state models depends upon insights and assumptions closely tied to the structure of both the full-scale INS error model and the measurement error model. First, the generally accepted nine-state model of INS error characteristics, in which position, velocity, and attitude error about three coordinate directions (east, north, up) are totally intercoupled,[2-4] can be partitioned according to the state subsets $(\delta x_e, \delta v_e, \phi_n)$, $(\delta x_n, \delta v_n, \phi_e)$, ϕ_u, and $(\delta x_u, \delta v_u)$. The last set is only weakly coupled to the first seven states, and in fact is totally decoupled from them if the vehicle were at rest and the Earth were nonrotating. Moreover, the errors in this vertical channel are kept suitably small with altimeter aiding external to the filter, so these two states are ignored.

Under the same assumption of the vehicle at rest on a nonrotating Earth, the first three sets of states also decouple, with the first two being characterized by Schuler oscillations and depicted as in Eq. (1). When the vehicle-centered east-north-up frame moves over a rotating Earth, response mode modification and intercoupling occur. But the error oscillations are still Schuler dominated since the Schuler angular rate $\sqrt{g/R_0}$ is significantly greater than coupling terms on the order of Earth rate Ω relative to inertial space and vehicle position angular rate relative to the Earth (i.e., velocity component divided by R_0); and Schular rate squared dominates vehicle position angular accelerations. Cross coupling occurs among the three attitude error states predominantly due to nonzero Earth rate and vehicle velocity, and the rate of change of velocity error states couple into those attitude errors through nonzero specific force. For instance, terms to be added to the right-hand side of Eq. (1) include

$$\begin{bmatrix} 0 & 0 & 0 \\ 0 & -(f_u - g) & f_n \\ -\omega_u & 0 & \omega_e \end{bmatrix} \begin{bmatrix} \phi_e \\ \phi_n \\ \phi_u \end{bmatrix}$$

where f_u and f_n are specific force components, and ω_u and ω_e are components of angular rate of the east-north-up frame with respect to inertial space; additional cross-coupling effects also develop among the nine error states. The uncertainties w_{e1} and w_{e2} in Eq. (1) partially account for these neglected terms, though in a rather crude manner. Were it not for the severe computer memory restriction, more explicit incorporation of these effects and inclusion of the azimuth error state ϕ_u would warrant attention as a means of enhancing performance. Especially for the application envisioned here, in which flight is along a rather benign glide trajectory, the simplistic model given in Eq. (1) might well suffice.

Decoupling into two separate filters also requires that the measurements introduce no nonnegligible cross coupling. In fact, the measurement gradient matrix $\boldsymbol{H}$ associated with the full-scale INS error model does not intercouple the two horizontal channels with each other or the vertical channel. Moreover, if $v_1(t_i)$ and $v_2(t_i)$ are the measurement noises associated with east and north position differences, as in Eqs. (6) and (7), then the equiprobability ellipsoids for the vector $[v_1(t_i)\ v_2(t_i)]^T$ must either have their principal axes aligned with the reference coordinate directions or be (nearly) circular, so that there is no cross correlation to intercouple the two horizontal channels. This poses no difficulty for this particular problem.

The Kalman filter based upon a model described by Eqs. (2),(3),(7) and (8) generates a state estimate $\hat{\boldsymbol{x}}(t_i^+)$ and associated error covariance matrix $\boldsymbol{P}(t_i^+)$ at time t_i after incorporating the measurement $z(t_i)$, in terms of the estimate $\hat{\boldsymbol{x}}(t_i^-)$ and covariance $\boldsymbol{P}(t_i^-)$ before measurement incorporation, through:

$$\boldsymbol{K}(t_i) = \boldsymbol{P}(t_i^-)\boldsymbol{H}^T[\boldsymbol{H}\boldsymbol{P}(t_i^-)\boldsymbol{H}^T + R(t_i)]^{-1} \tag{9}$$

$$\hat{\boldsymbol{x}}(t_i^+) = \hat{\boldsymbol{x}}(t_i^-) + \boldsymbol{K}(t_i)[z(t_i) - \boldsymbol{H}\hat{\boldsymbol{x}}(t_i^-)] \tag{10}$$

$$\boldsymbol{P}(t_i^+) = \boldsymbol{P}(t_i^-) - \boldsymbol{K}(t_i)\boldsymbol{H}\boldsymbol{P}(t_i^-) \tag{11}$$

To propagate to the next sample time, t_{i+1}, the relations are

$$\hat{\boldsymbol{x}}(t_{i+1}^-) = \boldsymbol{\Phi}(t_{i+1} - t_i)\hat{\boldsymbol{x}}(t_i^+) \tag{12}$$

$$\begin{aligned} \boldsymbol{P}(t_{i+1}^-) &= \boldsymbol{\Phi}(t_{i+1} - t_i)\boldsymbol{P}(t_i^+)\boldsymbol{\Phi}^T(t_{i+1} - t_i) \\ &\quad + \int_{t_i}^{t_{i+1}} \boldsymbol{\Phi}(t_{i+1} - t)\boldsymbol{G}\boldsymbol{Q}\boldsymbol{G}^T\boldsymbol{\Phi}^T(t_{i+1} - t)\,dt \end{aligned} \tag{13}$$

where $\boldsymbol{\Phi}$ is the state transition matrix satisfying $\dot{\boldsymbol{\Phi}} = \boldsymbol{F}\boldsymbol{\Phi}$ with initial condition $\boldsymbol{\Phi}(0)$ equal to the identity matrix $\boldsymbol{I}$. This filter recursion is started from the initial conditions

$$\hat{\boldsymbol{x}}(t_0) = \hat{\boldsymbol{x}}_0 = \text{assumed value (zero vector)} \tag{14}$$

$$\boldsymbol{P}(t_0) = \boldsymbol{P}_0 = \text{assumed value} \tag{15}$$

where $\hat{\boldsymbol{x}}_0$ and $\boldsymbol{P}_0$ characterize a Gaussian random vector model for a priori state knowledge.

To specify the filter algorithm completely, the dynamic noise strength $\boldsymbol{Q}$ in Eqs. (3) and (13), the measurement noise strength time history $R(t_i)$ in Eqs. (8) and (9), and the initial state covariance $\boldsymbol{P}_0$ in Eq. (15) must be established for both filters. Finding the best such values iteratively through a performance analysis of the resulting algorithms is the process of filter tuning and will be discussed subsequently.

Covariance Analysis of Performance

Figure 1 portrays the basic concept of a filter performance analysis.[5] In actual operation, the filter (the two 3-state filters can be viewed as a single decoupled 6-state filter) is driven by measurements $z(t_i)$ from INS and RAC hardware, and provides estimates of the states, $\hat{\boldsymbol{x}}(t_i)$, which are used as

corrective feedback to the INS. For analysis purposes, the "real world" environment is replaced by a "truth model," a large-dimensioned (46 or 61 states in this case, depending on which INS is used) state model that describes the characteristics of the "real world" measurements very accurately. Since this is a mathematical model, one can also extract from it a representation of the "true" values of quantities being estimated in the filter, denoted as $\boldsymbol{x}(t_i)$. In this case, $\boldsymbol{x}(t_i)$ is simply six of the states in the "truth model" itself.

An error vector $\boldsymbol{e}(t_i)$ can be formed as the difference of the true $\boldsymbol{x}(t_i)$ and the estimated $\hat{\boldsymbol{x}}(t_i)$. A statistical characterization of this error vector then delineates the actual performance capabilities of the filter. This can be accomplished by a Monte Carlo analysis, in which many samples of the stochastic process $\boldsymbol{e}$ are generated, and then sample statistics are generated as ensemble averages. However, in this case the truth model is adequately described in the form of a linear system driven by white Gaussian noises, so the covariance of $\boldsymbol{e}(t_i)$ can be computed directly through a single run of a covariance recursion instead. This method was used to generate time histories of filter rms errors.

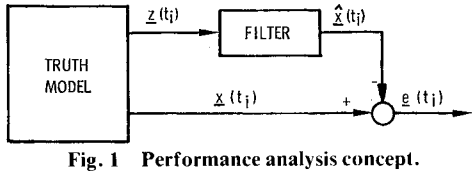

Fig. 1 Performance analysis concept.

"Truth Model" Development

The truth model required in the performance analysis can be described by

$$\dot{\boldsymbol{x}}_t(t) = \boldsymbol{F}_t(t)\boldsymbol{x}_t(t) + \boldsymbol{w}_t(t) \tag{16}$$

$$\boldsymbol{z}_t(t_i) = \boldsymbol{H}_t\boldsymbol{x}_t(t_i) + \boldsymbol{v}_t(t_i) \tag{17}$$

Table 1 presents the 46 states of the truth model for the laser gyro system[2,6-8] and the 61 states corresponding to the conventional gyro system.[2,9] Associated with each state are its initial variance (appropriate $\boldsymbol{P}_{t0}$ diagonal term) and white driving noise strength ($\boldsymbol{Q}_t$ diagonal term); both $\boldsymbol{P}_{t0}$ and $\boldsymbol{Q}_t$ are assumed to be diagonal. For states that are modeled as first-order Markov processes (outputs of first-order lags driven by white noise), the $\boldsymbol{Q}_t$ term is described in terms of the $\boldsymbol{P}_{t0}$ term and correlation time T in such a manner as to yield stationary processes.

The first nine states are the variables used to describe the error characteristics of an INS. Although each INS under consideration is a strapdown system, this error model can be

Table 1 Truth model state description

State	Laser gyro INS system $\boldsymbol{P}_{t0}$ term	Laser gyro INS system $\boldsymbol{Q}_t$ term	Conventional gyro INS system $\boldsymbol{P}_{t0}$ term	Conventional gyro INS system $\boldsymbol{Q}_t$ term
Basic INS:				
Position errors (3)	$(1500\text{ ft})^2$	0	$(1500\text{ ft})^2$	0
Velocity errors (3)	$(2\text{ ft/s})^2$	0	$(2\text{ ft/s})^2$	0
Attitude errors (3)	$(0.5\text{ millirad})^2$	7.6×10^{-11} rad^2/s	$(0.5\text{ millirad})^2$	0
Accelerometers:				
Accelerometer biases (3) (day-to-day nonrepeatability)	$(250\mu g)^2$	0	$(200\mu g)^2$	0
Accelerometer scale factor errors (3)	$(500\text{ ppm})^2$	0	$(405.6\text{ ppm})^2$	0
Accelerometer input axis misalignments (6)	$(10\text{ arc-s})^2$	0	$(30\text{ arc-s})^2$	0
Accelerometer biases (3) ($T_1 = 60$ min)	$(40\mu g)^2$	$2P_{t0}/T_1$	$(60\mu g)^2$	$2P_{t0}/T_1$
Accelerometer biases (3) ($T_2 = 15$ min)	$(20\mu g)^2$	$2P_{t0}/T_2$	$(30\mu g)^2$	$2P_{t0}/T_2$
Gravity knowledge:				
Gravity deflections (2) ($d_1 = 10$ n. mi.)	$(26\mu g)^2$(east) $(17\mu g)^2$(north)	$2P_{t0}v/d_1$	$(26\mu g)^2$(east) $(17\mu g)^2$(north)	$2P_{t0}v/d_1$
Gravity anomaly (1) ($d_2 = 60$ n. mi.)	$(35\mu g)^2$	$2P_{t0}v/d_2$	$(35\mu g)^2$	$2P_{t0}v/d_2$
Gyros:				
Gyro drift rate biases (3)	$(0.09\text{ deg/h})^2$	1.47×10^{-18} rad^2/s^3	$(2.0\text{ deg/h})^2$(roll axis) $(1.33\text{ deg/h})^2$(other two)	0
Gyro scale factor errors (3)	$(100\text{ ppm})^2$	0	$(500\text{ ppm})^2$	0
Gyro input axis misalignments (6)	$(6\text{ arc-s})^2$	0	$(30\text{ arc-s})^2$	0
Gyro drift rate (3) ($T_1 = 60$ min)	. . .	. . .	$(0.4\text{ deg/h})^2$(*oav*) $(0.6\text{ deg/h})^2$(*iav*)	$2P_{t0}/T_1$
Gyro drift rate (3) ($T_2 = 15$ min)	. . .	. . .	$(0.2\text{ deg/h})^2$(*oav*) $(0.3\text{ deg/h})^2$(*iav*)	$2P_{t0}/T_1$
g-sensitive drift coefficients (6)	. . .	. . .	$(2.0\text{ deg/h/}g)^2$	0
g^2-sensitive drift coefficients (3)	. . .	. . .	$(0.1\text{ deg/h/}g^2)^2$	0
RAC:				
RAC biases (2)	P_{ba}(along-track) P_{bc}(cross-track)	0	P_{ba}(along-track) P_{bc} (cross-track)	0
Altimeter:				
Altimeter bias (1) ($d = 250$ n. mi.)	$(500\text{ ft})^2$	$2P_{t0}v/d$	$(500\text{ ft})^2$	$2P_{t0}v/d$
Altimeter scale factor error (1)	$(0.03)^2$	0	$(0.03)^2$	0

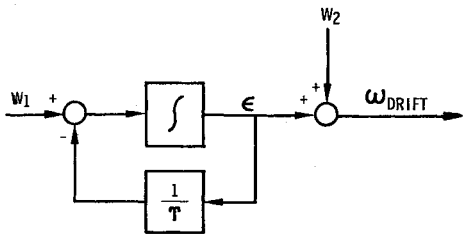

Fig. 2 Gyro drift rate model.

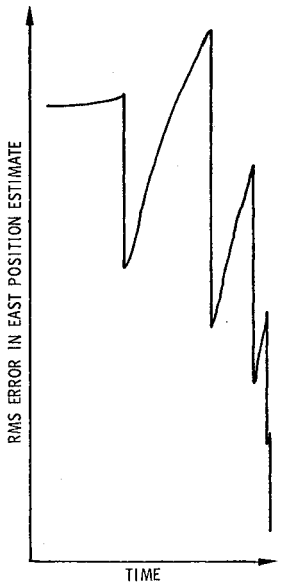

Fig. 3 rms error in east position estimate.

expressed conveniently with respect to an east-north-up coordinate frame.[2] The Q_t terms associated with attitude errors are due to gyro drift and will be discussed subsequently.

Accelerometer errors are described by means of a day-to-day nonrepeatability bias, scale factor error, two input axis misalignments, and two first-order Markov process states for each accelerometer. Uncertainty in the knowledge of gravity also enters the truth model state equations at the acceleration level. The errors between the true geoid and the assumed ellipsoid for INS navigation computations have been described by means of first-order Markov process models,[2] with mean square values and correlation distances as described in Table 1. If a correlation distance is denoted as d and the vehicle velocity magnitude as v, a corresponding correlation time is generated as $T=d/v$, thereby yielding the Q_t term expression in the table.

Gyro errors are depicted by a drift rate bias state (or Brownian motion state for the laser gyro), scale factor error, two input axis misalignments, two first-order Markov process states, two g-sensitive drift coefficients (spin and input axes), and one g^2-sensitive drift coefficient (major spin-input coefficient) for each gyro. For the laser gyros, only the first four of these nine states are included, since the others are essentially nonexistent. Another marked difference from conventional gyros is embodied in the drift rate model. Figure 2 displays a typical gyro drift rate model, composed of first-order Markov process ϵ (in the limit of very long correlation time T, this becomes a Brownian motion model) and an additive, independent white Gaussian noise w_2. In conventional gyros, the ϵ contribution to drift rate dominates w_2, and the latter is often neglected. However, for laser gyros, the effect of w_2 predominates; its noise strength is given by the Q_t terms driving INS attitude errors in Table 1. A final difference of the two gyro types is the set of multiple table entries for certain conventional gyro states. On the Markov process states, *oav* denotes output axis vertical, while *iav* means input axis vertical. The roll axis gyro drift rate bias entry is higher than the others because a different gyro design is employed to withstand and indicate the larger range of rates that can occur about this axis. In the laser gyro INS, the gyro sensitive axes are canted off from the vehicle body axes to distribute high roll rates among three identical gyros.

Although Table 1 shows accelerometer errors to be very similar in the two inertial systems, the gyro characteristics are significantly worse in the conventional gyro INS. The low-frequency power spectral density value of ω_{DRIFT} described in Fig. 2 is three orders-of-magnitude larger in the conventional unit. Moreover, drift rate biases, scale factor errors, and misalignments are considerably greater; and the g and g^2 errors have no counterpart in the laser gyro system.

The errors in the RAC data are modeled as a corruptive white Gaussian noise plus a bias. This is a necessarily unsophisticated model of RAC error characteristics, since only sparse and incomplete performance data were available at time of truth model development. Nevertheless, these data were sufficient to estimate appropriate noise strengths and to indicate that bias effects were not negligible. The strength of the two-dimensional white noise, v_t in Eq. (17), was found to be well modeled as

$$R_t(t_i) = [\theta \cdot h(t_i)]^2 I \tag{18}$$

where $h(t_i)$ is the vehicle altitude and θ is a parameter with classified numerical value. Each bias was modeled as a random constant with mean zero and variance as shown in Table 1, again the numerical values being classified. Although physical reasoning could lead to altitude-dependent variances on the bias states as well, the available data were not consistent or complete enough to warrant this formulation. Because high statistical confidence could not be placed in this model, a study of performance sensitivity to bias model parameter variations was deemed essential; this will be discussed further in the next section.

Finally, the altimeter errors are described in terms of a first-order Markov process noise plus a scale factor error. The altimeter is used to damp out the inherently unstable vertical errors in the INS, and so its errors drive certain INS error states in the truth model.

Analysis Results

The covariance analysis technique was first used to tune the proposed filter for use in each of the two INS/RAC system configurations.[6,9,10] The filters' P_0 and time histories of Q and R were iteratively modifed to yield minimum rms values of the estimation error e components for all time of interest. For this application, terminal position errors are especially important, but the entire history of all errors must be considered to preclude being outside the bounds of a prestored RAC map at an update time and to insure sending proper corrective control commands during the terminal phase of flight.

Figure 3 plots the rms error (in log scale) in the east position estimate provided by the filter tuned to the laser gyro system. To aid the tuning process, it is useful to compare these "actual" rms errors with the filter's own representation of its errors – its own computed covariance P. If the filter underestimates its own errors relative to those in subsequent measurements, it will not "look hard enough" at the measurements (possibly causing divergence problems), whereas if it overestimates its own errors, then it expends too much effort tracking noisy data and does not exploit its internal model enough. Despite the simple filter form and the fact that a constant Q is used for all time, the filter-computed rms error history essentially duplicates the results shown in Fig. 3. Moreover, this condition does effectively yield the best estimate precision. The results for the other five filter states, and those for the conventional gyro system, are very similar.

Table 2 Error budget

Error source removed	% of terminal rms nav errors: Laser gyro INS	Conventional INS
None (baseline)	100	100 (= 107.5% of laser error)
Accel errors	100	99.9
Gyro errors	100	98.1
Initial condition	100	100.0
RAC bias	95	96
All RAC errors	9	11

For computational simplicity, it was proposed to approximate the integral term in Eq. (13) by a diagonal matrix.[1] The original such design was found to be severely out of tune, and even the best tuning achievable with a diagonal matrix form yielded noticeably degraded performance. The degradation was naturally least in the channels for which direct measurements were available, i.e., position errors, and these are the estimates of primary interest for this application. However, the computation of three off-diagonal terms in a symmetric 3×3 matrix is not burdensome. Moreover, a followup study[11] has indicated a substantial increase in importance of these off-diagonal terms for obtaining good performance along more highly dynamic trajectories with optimized measurement sample times. Therefore, weapon system development and testing is continuing at the Air Force Armament Laboratory with the design changed to incorporate these terms.

An error budget was generated to depict the contributions of individual error sources to the rms errors throughout the vehicle flight. Once the filter was tuned, repeated covariance analyses were conducted, each with a single error source removed.[6,9,10] Table 2 presents the results for rms position errors at the terminal time. From this table, it is evident that the RAC errors have the greatest influence on estimate precision at the terminal time. This is caused by the extreme accuracy of low-altitude RAC position fixes and the fact that the last two fixes are taken shortly before the end of flight to maximize the benefit of the limited number of updates. Error budgets for estimation errors earlier in the flight reveal an increased importance of INS sensor errors.

Table 2 also reveals that the laser gyro INS configuration outperforms the conventional gyro system, as would be predictable from relative precision of instruments as described in Table 1. Also, the white noise gyro drift rate model in the filters is appropriate for a laser gyro, whereas a first-order Markov process model, requiring an additional state per filter, would be a significantly better model for a conventional gyro. The table also shows that the gyro errors in the conventional INS system play a more dominant relative role in degrading performance than the same errors do in the laser gyro INS. These trends are accentuated at earlier times in the flight, especially in the case of dynamic trajectories.

Because of the significance of RAC errors and the sparse amount of test data concerning bias errors in this device, the sensitivity of estimation accuracy to varying bias levels was analyzed. Table 3 demonstrates the effect of varying the RAC bias variance from zero to four times the value listed in Table 1. These results and those depicted in Table 2 reveal that, if performance requirements are not met, seeking a better RAC system would be more beneficial than improving the INS precision. Similarly, if the filter complexity could be increased, it would be most advantageous to incorporate a better model for the errors in the RAC system position data.

Table 3 Sensitivity to RAC bias

RAC bias model standard deviation	% of terminal rms nav errors: Laser gyro INS	Conventional INS
0	95	96
standard	100	100
2 × standard	113	119

Direct estimation of RAC biases by adding a fourth state to each filter is not feasible: adding the model $\dot{b}=w_3$ to Eq. (1), and modifying Eq. (6) to let z be (δx_e+b+v), yields an unobservable system model. Basically, the filter would not be able to provide valid estimates of δx_e and b separately. Improved estimation performance can be achieved by replacing Eq. (18) with

$$R(t_i)=\{[\theta\cdot h(t_i)]^2+R_b(t_i)\}I \tag{19}$$

in the filter formulation, where R_b scales with the variance of the RAC bias in the truth model. Although bias errors are not directly compensated, the better model for rms measurement errors yields more proper weighting of update information, and thus enhanced performance. However, these conclusions are based upon the adequacy of the truth model depiction of RAC errors. Once enough performance data are analyzed to have statistical confidence in the RAC error model, the preceding modification and other means of enhancement can be fully exploited in the operational filter.

Conclusion

Because of severe restrictions on computer time and memory allotted, a very simple Kalman filter was designed to update a strapdown inertial system with position fixes from a radiometric area correlator. Nevertheless, its performance has been analyzed and found to meet specifications. System development and testing is continuing. Current efforts include investigation of exploiting square root or $U-D$ covariance factorizations[5,12,13] to counter the numerical precision and stability problems of Kalman filters implemented on a short wordlength computer.

References

[1] "Position Update Filter Function," Radiometric Area Correlation Guidance Captive Flight Test R&D Status Rept., Oct. 1975; Lockheed Missiles and Space Co., Inc., Sunnyvale, Cal., LMSC-D434550, Nov. 1975.

[2] Widnall, W.S. and Grundy, P.A., "Inertial Navigation System Error Models," Intermetrics, Inc., Cambridge, Mass., TR-03-73, May 1973.

[3] Pinson, J.C., "Inertial Guidance for Cruise Vehicles," *Guidance and Control of Aerospace Vehicles,* edited by C.T. Leondes, McGraw-Hill, New York, 1963.

[4] Britting, K.R., *Inertial Navigation System Analysis,* John Wiley and Sons, New York, 1971.

[5] Maybeck, P.S., *Stochastic Models, Estimation and Control,* to be published, Academic Press, 1978; also "Applied Optimal Estimation: Kalman Filter Design and Implementation," Air Force Institute of Technology, Wright-Patterson Air Force Base., Ohio, Short Course Notes, 1975.

[6] Maybeck, P.S., "Covariance Analysis of a Laser-Gyro INS/Radiometric Area Correlator (RACG) System Kalman Filter Design," Wright-Patterson Air Force Base, Ohio, AFIT-TR-76-13, Feb. 1976 (confidential).

[7] Morrison, R., Garret, H., and Walls, B., "A Strapdown Laser Gyro Navigator," *IEEE National Aerospace and Electronic Conference,* Dayton, Ohio, May 1974.

[8]Pasik, D.J., Gneses, M.I., and Taylor, G.R., "A Ring Laser Gyro Strapdown Inertial Navigation System: Performance Analysis and Test Results," AIAA Paper 75-1095, Boston, Mass., Aug. 1975.

[9]Maybeck, P.S., "Covariance Analysis of a Kalman Filter for a Conventional-Gyro Strapdown INS/Radiometric Area Correlator Guidance System," Wright-Patterson Air Force Base, Ohio, AFIT-TR-76-14, July 1976 (confidential).

[10]Maybeck, P.S., "Analysis of a Kalman Filter for a Strapdown Inertial/Radiometric Area Correlator Guidance System," *Proceedings of the 1977 IEEE National Aerospace and Electronics Conference,* Dayton, Ohio, May 1977.

[11]Fitschen, C.K., "Covariance Analysis of Kalman Filters Proposed for a Radiometric Area Correlation/Inertial Navigation Guidance System," MS Thesis, Air Force Institute of Technology, Wright-Patterson Air Force Base, Ohio, Dec. 1976.

[12]Bierman, G.J., "Measurement Updating Using the U-D Factorization," *Proceedings of the 1975 IEEE Conference on Decision and Control,* Houston, Texas, Dec. 1975.

[13]Thornton, C.L., and Bierman, G.J., "Gram-Schmidt Algorithms for Covariance Propagation," *Proceedings of the 1975 IEEE Conference on Decision and Control,* Houston, Texas, Dec. 1975.